ELSEVIER

Contents lists available at ScienceDirect

Composite Structures

journal homepage: www.elsevier.com/locate/compstruct





Multi-functional application of recycled carbon fibres in hybrid composites for notch sensitivity reduction and damage monitoring

Fan Zhang a,b,*, Ting Yang Ling bo, Liudi Jiang co, Yonggang Zhang d, Khong Wui Gan ao

- ^a Smart Manufacturing and Systems Research Group, University of Southampton Malaysia, 79100 Iskandar Puteri, Johor, Malaysia
- b School of Electronics and Computer Science, Faculty of Engineering and Physical Sciences, University of Southampton, Southampton SO17 1BJ, United Kingdom
- c School of Engineering, Faculty of Engineering and Physical Sciences, University of Southampton, Southampton SO17 1BJ, United Kingdom
- ^d National Engineering Laboratory of Carbon Fiber Preparation Technology, Ningbo Institute of Material Technology and Engineering, Chinese Academy of Sciences, Ningbo, Zhejiang 315201, China

ARTICLE INFO

Keywords: Recycled carbon fibre Hybrid composites Notched strength Multifunctional composites

ABSTRACT

It is challenging to reuse recycled carbon fibres (rCF) alone as reinforcement material in composites for structural application due to its discontinuous and non-aligned fibre architecture. This study investigates innovative usage of rCF when hybridized with other reinforcement fibres in a hybrid composite for multi-functional application. A rCF non-woven is embedded in an E-glass fabric composite laminate to demonstrate its multi-functionality in open-hole specimens with various hole sizes under monotonic tensile loading. Instead of brittle failure, the rCF fails in a progressive manner due to the in-situ effect offered by the neighbouring glass fibre sublaminates. Following damage initiation in the rCF layer, delamination takes place along the rCF and glass fabric interfaces, enabling stress redistribution around the hole. This leads to reduced stress concentration, resulting in a notch-insensitive hybrid composite when compared to the non-hybrid glass fabric composite. By monitoring the change in electrical resistance of the rCF layer, the progressive damage events around the hole can be inferred. Regardless of the hole size, a simple damage self-sensing system can be developed to inform the damage severity of the hybrid composite. In this study, the rCF layer gives a damage tolerant notched composite and simultaneously offers damage monitoring functionality.

1. Introduction

Carbon fibres have been widely exploited to manufacture advanced composites for applications in aerospace, automotive, marine, energy and construction industries, owing to their exceptional strength-to-weight ratios. However, they are also known to be expensive and energy-intensive to produce with an embodied energy of 183–286 MJ/kg, compared with 13–32 MJ/kg and 110–210 MJ/kg for glass fibres and stainless steel respectively [1]. It also raises the waste management issue when these composite components reach their end of life as recycling and reusing them is not as straightforward as their metallic counterpart. The last two decades have seen the development and commercialisation of various technologies to recover the valuable carbon fibres from composite waste, which can be found in the form of manufacturing scraps or end-of-life composite components [2]. Recycled or reclaimed carbon fibres are generally discontinuous, non-aligned and entangled, resulting in significant depreciation in structural performance compared

to virgin continuous carbon fibres. There is also a lack of confidence in the quality of recycled carbon fibres (rCF) as they could previously come from various manufacturing processes and service backgrounds without historic data or information. Currently there is limited research work focusing on how to best reuse the rCF in high-value applications, with a view to addressing the challenge to establish a sustainable circular economy.

Despite their reduced mechanical performance as compared with virgin CFs, short discontinuous rCF could still be used for structural applications if they are incorporated into conventional composite laminates at low fibre loading, which can enhance the mechanical properties of the composites. Attahu et al. [3] showed that the unidirectional carbon fibre/epoxy laminate with a single core layer of low areal density $(60~{\rm g/m^2})$ rCF non-woven mat gives better flexural and damping performance than that with a virgin aramid fibre mat. Koçoğlu et al. [4] reported improvement of 60~% and 30~% in flexural and tensile strength respectively when $12~{\rm mm}$ scrap carbon fibres at 6.7~% fibre volume

^{*} Corresponding author at: Smart Manufacturing and System Research Group, University of Southampton Malaysia, 79100 Iskandar Puteri, Johor, Malaysia. E-mail address: fz1y22@soton.ac.uk (F. Zhang).

fraction were added to the hot-pressed glass fabric/polyamide composite. The study by Quan et al. [5] used rCF for interlayer toughening of carbon fibre/epoxy composites, showing that fracture toughness can be improved by 17 % and 66 % for Mode I and Mode II fracture initiation energy respectively.

Recent literature also suggests that rCF can be incorporated into cementitious composites for infrastructure construction as aggregate replacement or as reinforcing material, but with mixed results depending on numerous factors such as rCF length, dispersion of rCF, surface treatment of rCF, impurities etc. [6] In general, there is improvement in tensile behaviour of cementitious composites when a small amount of rCF (around 1 % by volume or 2 % by weight) was added to them [7,8]. Mastali et al. [9] observed that increasing the length and dosage of rCF increases the impact resistance of rCF reinforced self-compacting concrete. Making use of their excellent electrical properties, Segura et al. [10] mixed rCF in concrete to modify its conductive characteristic to develop smart self-sensing cementitious materials for civil engineering structural health monitoring. Belli et al. [11] also reported that the addition of rCF (up to 1.6 % by volume) in cement mortars is able to improve their electrical conductivity up to one order of magnitude, while increasing their flexural and tensile splitting strength up to 100 %. Other novel application of rCF includes its use as the electromagnetic interference shielding material [12]. The findings above collectively demonstrate the potential of rCF as a sustainable multi-functional candidate material in improving mechanical as well as electrical properties of the composites. It is also cost-effective as rCF can be recovered from composite wastes at approximately 15 % of the cost of producing virgin carbon fibres from raw materials [13].

Large automobile manufacturers such as Chevrolet, BMW and Ford have demonstrated the potential of using rCF in large-scale manufacturing of body panels of cars [14]. More work remains to be done to develop and assess high-performance usage of rCF for future sustainability. It is challenging to process the rCF with short and discontinuous fibers. There are efforts to realign the random rCF to manufacture into semi-finished forms to improve fibre content and therefore mechanical performance via various additional dry or hydrodynamic processes [15–17]. Another straightforward way to reuse rCF is by bonding the fibres together mechanically or chemically to convert them into non-woven mats [18,19]. However, rCF non-wovens cannot be used alone as structural material due to their poor material properties and high material variability compared to the highly aligned continuous fibre architecture. Their drawback can be alleviated by using them together with other conventional composite plies to fabricate hybrid composite laminates. This paper aims to present innovative usage of rCF non-woven as a multi-functional material when embedded as a core layer in a E-glass fabric composite laminate to form a hybrid composite. The open-hole strength of a hybrid glass fibre/rCF composite with various hole sizes is investigated under monotonic tensile loading and compared with the non-hybrid composites to understand the role of rCF in reducing notch sensitivity. Concurrently the electrical resistance of the rCF layer in the specimens is measured in real time during loading and correlated to the progressive damage events taking place around the holes in order to demonstrate its damage monitoring capability. This merging of mechanical and structural health monitoring functions offers a new perspective of rCF as a sustainable solution to lightweight composite structures to meet the efficiency requirements in the energy and transportation industry.

2. Experimental methodology

2.1. Materials and specimen fabrication

A hybrid composite laminate was manufactured by sandwiching a rCF non-woven mat between two sublaminates. Each sublaminate comprises 4 plies of commercial-grade E-glass fibre fabric with plain weave fibre architecture. The rCF non-woven (CARBISO M IM56D) was

provided by ELG Carbon Fibre Ltd (now known as GEN 2 Carbon) in the form of a dry random mat with an areal density of 89 g/m², made from scrap intermediate modulus carbon fibres with sizing. Note that there is a small degree of anisotropy in the rCF non-woven due to the slight preferential fibre alignment in the weft direction during the manufacturing process of the non-woven fabric. The weft direction was chosen to be the loading direction in the lay-up. The areal density of a single ply of E-glass fibre fabric was 270 g/m². The fabrics were laid down on a flat aluminium caul plate and consolidated in a vacuum bag before being infused with epoxy resin (EpoxAmite 100) and finally cured in the room temperature for 24 h. For benchmarking purposes, two baseline non-hybrid laminates, consisting of 9 plies of the E-glass fibre fabric and 4 plies of rCF non-woven respectively such that they give the same number of plies or comparable thickness with the hybrid laminate, were also fabricated using the same resin system following the same procedures. This will allow comparative study of the mechanical behaviour and the hybrid effect between the non-hybrid and hybrid laminates. The stacking sequences of the three composite laminates are illustrated in Fig. 1.

The average thickness of the hybrid glass/rCF laminate was 2.19 mm, while the thickness of the non-hybrid glass fibre and rCF laminates were 1.81 mm and 2.37 mm respectively. Based on the density of the constituent materials and the areal density of the constituent layers, the fibre volume fraction of each laminate can be estimated as shown in Table 1. The three hybrid and non-hybrid laminates were then cut into specimens of 200 mm long and 20 mm wide using a water-cooled diamond wheel cutter. The specimen width of 20 mm was chosen to obtain across the width a round number of three repeating unit cells (about 6.7–6.8 mm in length per unit cell) of the plain weave architecture of the glass fibre fabric, such that representative test data of the fabric can be captured. 50 mm from both ends of the specimens were tabbed with glass fibre/epoxy, bonded with epoxy adhesive (Huntsmen Araldiate 2014–2), leaving a gauge section of 100 mm long.

2.2. Unnotched and open-hole tensile testing

Four specimens from each of the three laminates in Table 1 were selected for unnotched tensile testing to determine their unnotched mechanical properties, i.e. ultimate strength, effective stiffness and stress-strain relations. For the rest of the specimens of the hybrid glass/ rCF laminate and the non-hybrid glass fibre laminate, holes were made in the center using solid carbide dagger drill bits of various diameters to investigate their open-hole tensile behaviour and notch sensitivity. Four hole diameters of 2.4 mm, 3.2 mm, 4.1 mm and 5.95 mm were chosen, giving the hole diameter to specimen width (D/W) ratios 0.12, 0.16, 0.205 and 0.2975 respectively. To minimise delamination during drilling, a wooden backing plate was placed beneath the specimens. For the hole diameters larger than 3.2 mm, a smaller starter hole was made before enlarging it to the final diameter by incremental drilling. For the specimens of non-hybrid rCF laminate, only one hole diameter of 3.2 mm was investigated in this study for comparison purposes, as the mechanical performance of a pure rCF non-woven composite is not the main interest of this study. Three to four specimens were tested for each hole diameter for all laminates. Fig. 2 shows the overall dimensions of the unnotched and open-hole specimens.

All the unnotched and open-hole specimens were tested under monotonic tensile loading using a Shimadzu AGX-50kNV testing machine with a 50 kN load cell at a constant displacement rate of 1 mm/min at room temperature. The full-field displacement and strain fields of the specimens were acquired using a stereo Digital Image Correlation (DIC) set-up by capturing images at 2 Hz using a pair of Teledyne Flir 5 MP (2,448 \times 2,048 pixels) monochromatic Blackfly S cameras fitted with 50 mm focal length lenses. For the unnotched specimens, the cameras were positioned at 0.63 m away to capture the full gauge length with a stereo angle of 16.7°. For the notched specimens, the cameras were positioned at 0.34 m away with a stereo angle of 22.3° so that a

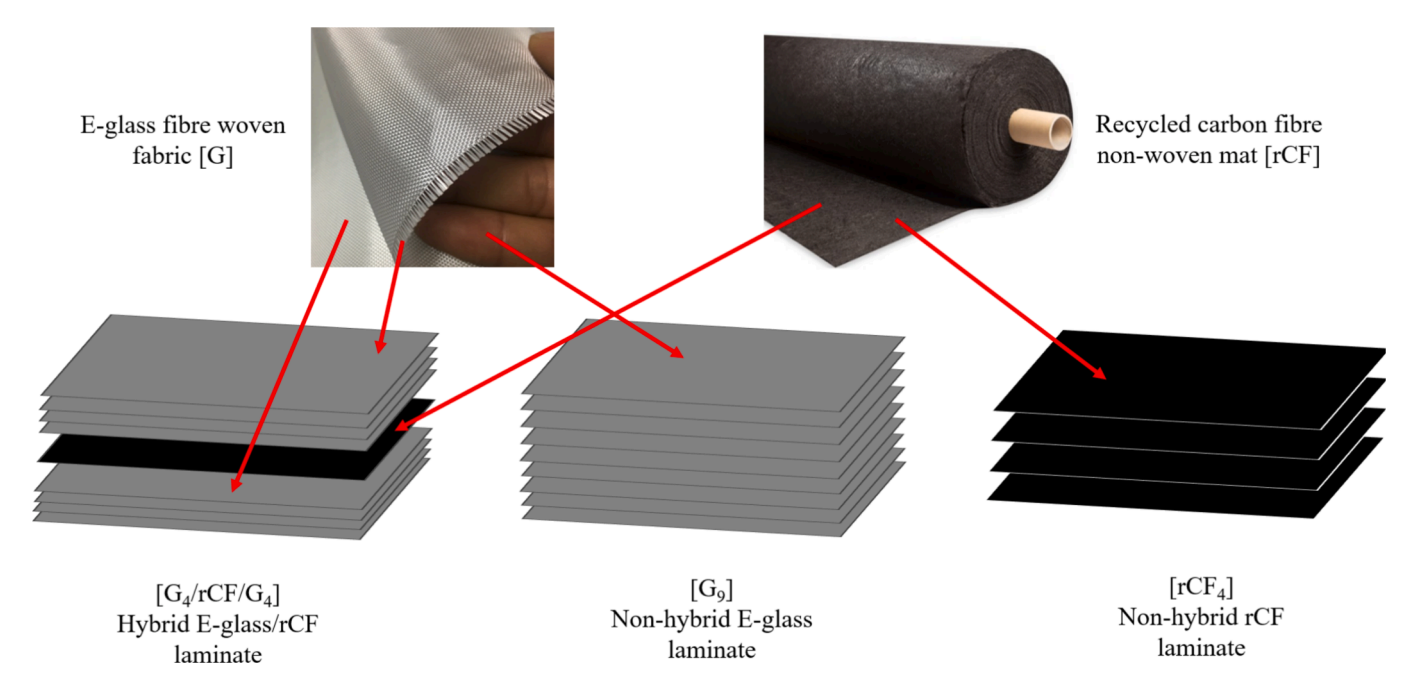


Fig. 1. Stacking sequence of hybrid E-glass/rCF laminate, non-hybrid E-glass laminate and non-hybrid rCF laminate.

Table 1Average thicknesses of the hybrid and non-hybrid laminates and their fibre volume fractions.

Laminate	Stacking sequence	Thickness (mm)	Areal density after resin infusion (g/ m ²)	Fibre volume fraction (%)	
				Glass fibre	Recycled carbon fibre
Hybrid E- glass/ rCF	[G ₄ /rCF/ G ₄]	2.19	3,674	38.5	2.7
Non- hybrid E-glass	[G ₉]	1.81	3,311	54.5	_
Non- hybrid rCF	[rCF ₄]	2.32	2,409	-	11.3

closer view on the deformation around the hole could be obtained. To prepare the specimens for DIC, one side of the specimens was first coated with white paint and then random black speckles were applied using air brush to control the speckle size and distribution such that there were approximately 3 to 5 speckles in the corresponding subsets. Images collected were analyzed using commercial software MatchID with subset and step sizes of 31 and 15 pixels respectively. For strain derivation, a strain window of 5 subsets (or datapoints) was used.

For the unnotched specimens, three virtual extensometers of 80 mm long along the longitudinal (loading) direction were placed each at three locations (left, middle and right across the specimen width) in the gauge section (Fig. 2a). The readings were averaged to obtain the global strain $\varepsilon_{xx,G}$ in the loading direction for establishing the global stress–strain relation. On the other hand, for all the open-hole specimens, two virtual extensometers of 30 mm long were placed close to both edges of the specimens and averaged to acquire the global strains $\varepsilon_{xx,G}$ away from the holes (Fig. 2b). A third virtual extensometer was positioned close to the edge of the hole to track the hole's edge-to-edge elongation in the loading direction. Two additional square regions of interest (ROIs) of 3.4 mm \times 3.4 mm were defined on both sides of the holes, within which strains in the loading direction were averaged to give the local strains ε_{xx} next to the holes. Comparison of the strain within the two ROIs is useful

to determine damage initiation and the extent of damage around the hole, which will be described in detail in Section 3.2. The size of the ROIs was chosen corresponding to the width of a single E-glass fibre tow in the plain weave fibre architecture. The gross stress and net stress of the open-hole specimens were calculated respectively as:

$$\sigma_{gross} = \frac{P}{W \bullet t} \tag{1}$$

and.

$$\sigma_{net} = \frac{P}{(W-D) \bullet t} \tag{2}$$

where P is the load, W is the specimen width, D is the hole diameter and t is the specimen thickness. The gross strength retention and net strength retention of the open-hole specimens can then be defined as the ratio of the gross strength and net strength of the open-hole specimens to those of the unnotched specimens respectively.

To demonstrate the structural health monitoring and damage sensing capability of the rCF layer around the hole under monotonic tensile loading, the electrical resistance change in the rCF layer in the hybrid composite was measured as a function of applied strain. The resistance was measured by four-point measurement to eliminate the contact resistance between the wires and the rCF layer. Four wires (two each on the upper and lower sides of the hole) as the electrodes were directly connected to the rCF layer along the same specimen edge using conductive silver paste. The arrangement of the electrodes on an openhole specimen (with hole diameter 3.2 mm) is shown in Fig. 3 (inset). The two outer electrodes were used to pass the current while the inner two were used for voltage measurement. To prevent detachment of the wires from the specimens during loading and to ensure stable reading, the wires were bonded on the specimen across the width using ultraviolet (UV) cured epoxy. The electrical resistance was measured by a digital multimeter (Keithley 2100) and recorded at a sampling rate of 20 Hz. The resistance reading was synchronized in time with the force measurement from the universal testing machine based on the timestamp provided by the computers. The full set-up of the tensile testing with the relevant instrumentation is illustrated in Fig. 3.

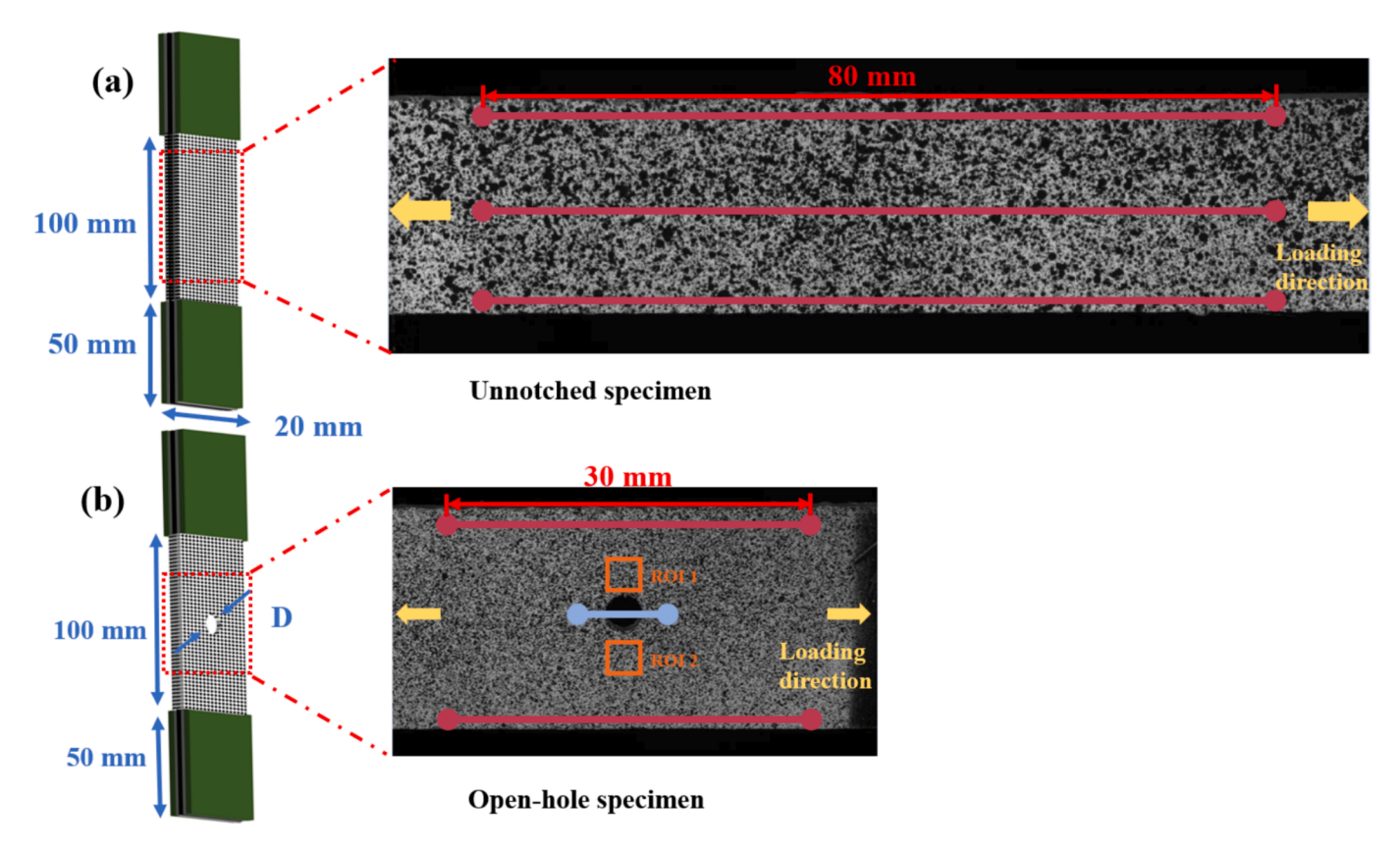


Fig. 2. (a) Unnotched specimen and the positioning of three virtual extensometers (shown as red lines) for global strain measurement. (b) Open-hole specimen and the positioning of two virtual extensometers (shown as red lines) for global strain measurement, one virtual extensometer (shown in blue) for hole elongation measurement and two square regions of interest (ROI 1 and ROI 2) for local strains measurement.

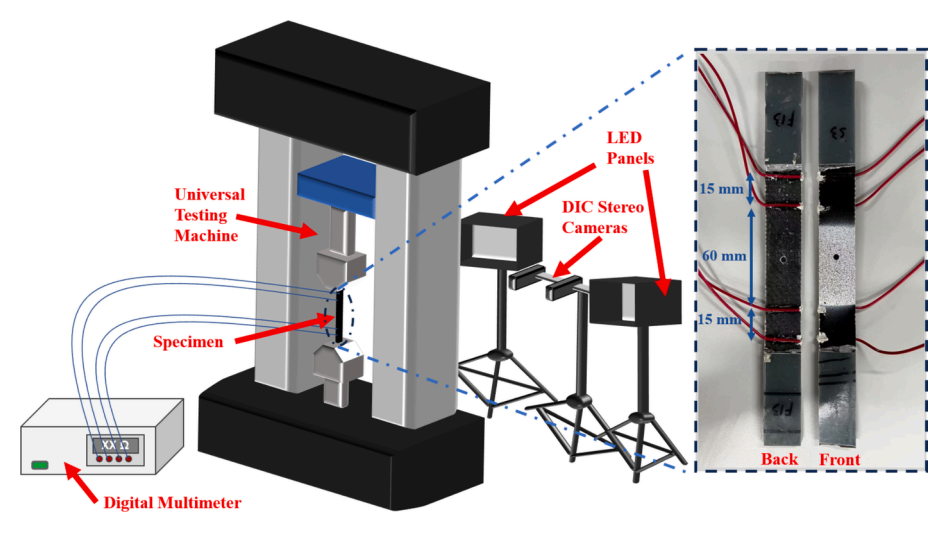


Fig. 3. Full experimental set-up of the tensile testing with digital image correlation for full-field strain measurement and a digital multimeter for electrical resistance measurement. (Inset) Front and back sides of a hybrid E-glass fibre/rCF composite specimen connected to 4 wires as the electrodes at the edge.

3. Experimental results and discussion

3.1. rCF for notch sensitivity reduction

This section demonstrates the role of rCF layer in enhancing the notch insensitivity of the hybrid composite. Performing the unnotched tensile tests provides the mechanical behaviour of the non-hybrid rCF and E-glass fibre composites such that they can be compared against the hybrid composite and provides the baseline data to the open-hole

specimens. Fig. 4 present the stress–strain curves of the non-hybrid rCF, non-hybrid E-glass fibre and their hybrid composite specimens respectively, with and without open holes. The stresses of the three laminates shown in the figures are given both in gross and net stresses. The strains used are global strains $\varepsilon_{xx,G}$ as described in Section 2.2. It should be noted that the apparent stiffer material responses of the notched specimens compared to the unnotched ones in Fig. 4b, 5b and 6b are simply an artefact due to the definition of global strain chosen for the open-hole specimens. The global strain was taken far away from the

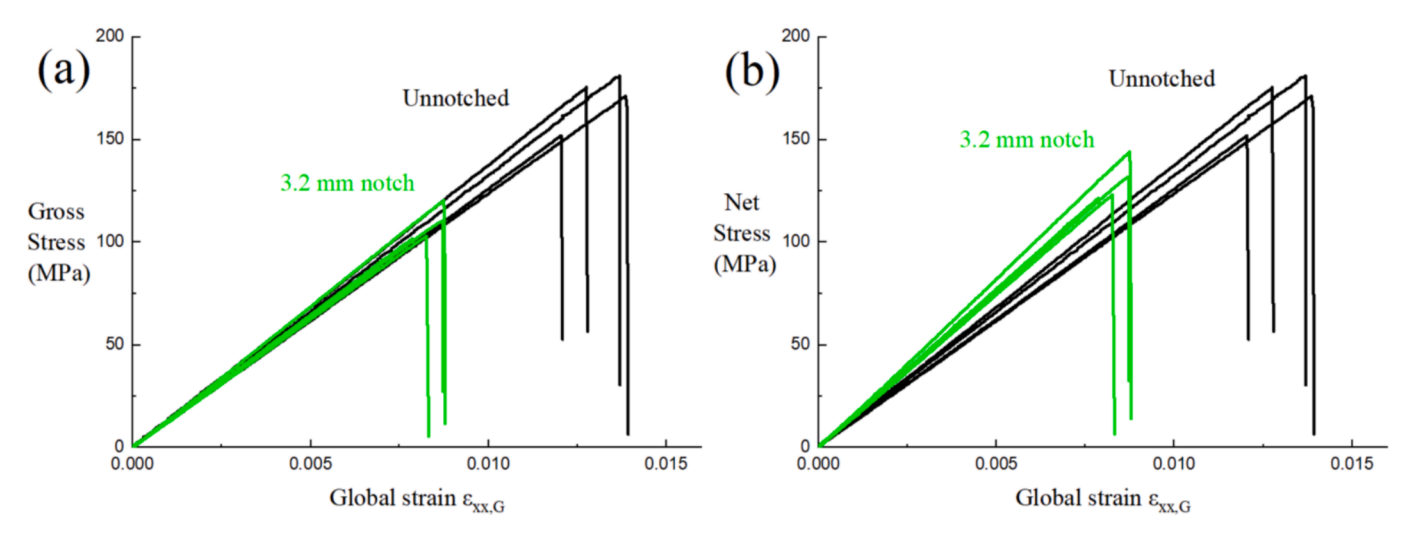


Fig. 4. (a) Gross and (b) net stress-strain curves of non-hybrid rCF composite unnotched specimens and open-hole specimens with a 3.2 mm-diameter hole.

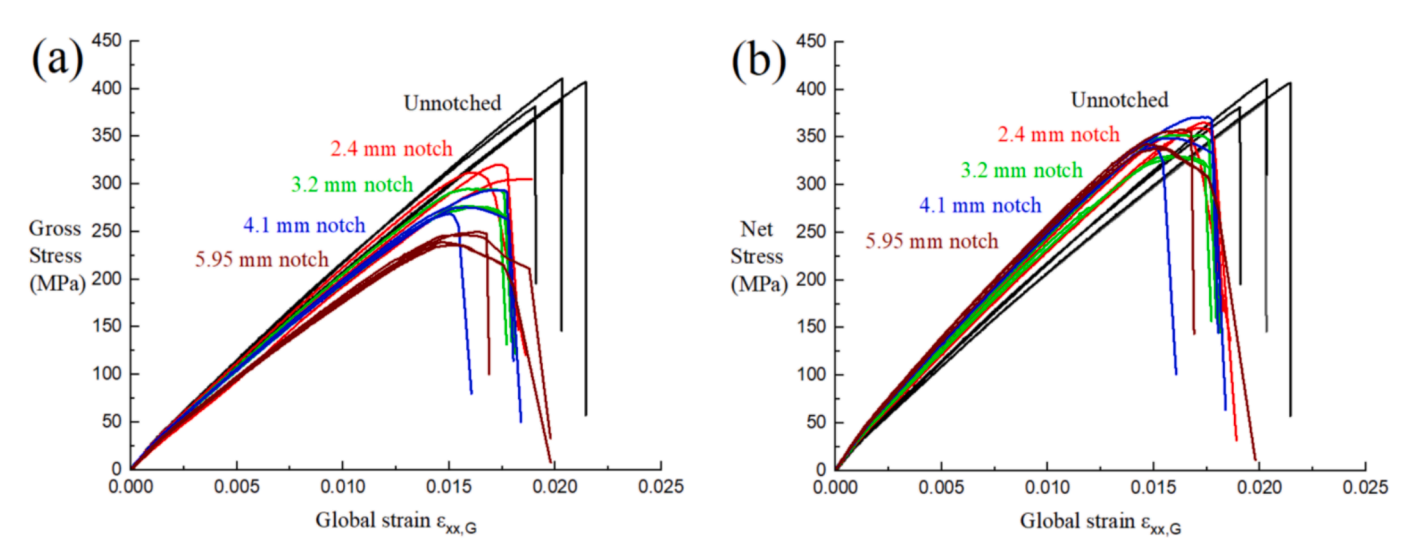


Fig. 5. (a) Gross and (b) net stress-strain curves of non-hybrid E-glass fibre composite unnotched specimens and open-hole specimens with various hole diameters.

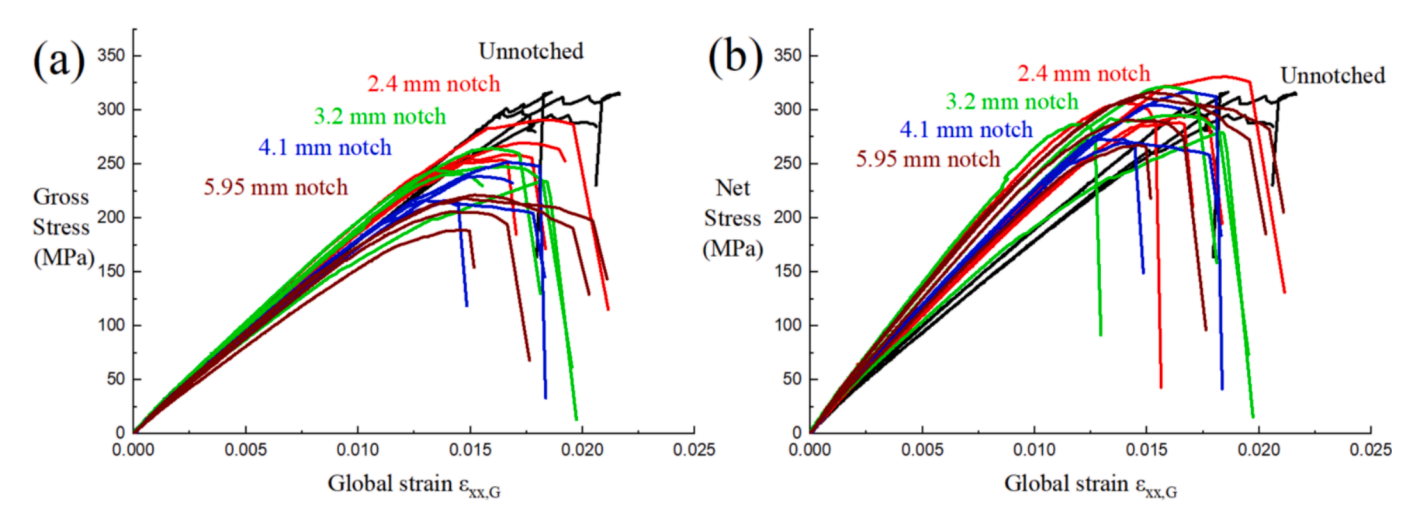


Fig. 6. (a) Gross and (b) net stress-strain curves of hybrid E-glass/rCF composite unnotched specimens and open-hole specimens with holes of various diameters.

hole and therefore lower than the average strain in the ligaments due to stress concentration, resulting in stiffer responses for the open-hole specimens. Table 2 shows the average maximum load and stress

achieved by each specimen configuration. Fig. 7 shows the failed openhole specimens of the three laminates with hole diameter 3.2 mm after tensile loading. Similar failure appearance was seen in the specimens of

Table 2Tensile test results of non-hybrid rCF, non-hybrid E-glass fibre and hybrid E-glass fibre/rCF composite specimens.

Laminate	Hole diameter (mm)	Maximum force (kN)	Maximum gross stress (c.v.) (MPa)	Gross strength retention (%)	Net strength retention (%)
Non- hybrid	Unnotched	8.11	175 (11.3 %)	-	_
rCF	3.2	5.26	114 (8.5 %)	64.8	80.8
Non-	Unnotched	14.40	397 (2.5 %)	_	_
hybrid	2.4	11.46	320 (2.6 %)	80.7	92.7
E-glass	3.2	10.15	283 (2.2 %)	71.4	87.4
	4.1	9.91	277 (2.8 %)	69.8	90.3
	5.95	8.64	241 (1.6 %)	60.8	90.6
Hybrid E-	Unnotched	13.73	301 (2.7 %)	_	_
glass	2.4	11.44	271 (4.2 %)	90.1	102.1
fibre/	3.2	10.84	246 (1.4 %)	81.6	97.6
rCF	4.1	9.81	228 (6.6 %)	75.8	96.3
	5.95	8.61	200 (5.3 %)	66.5	96.2

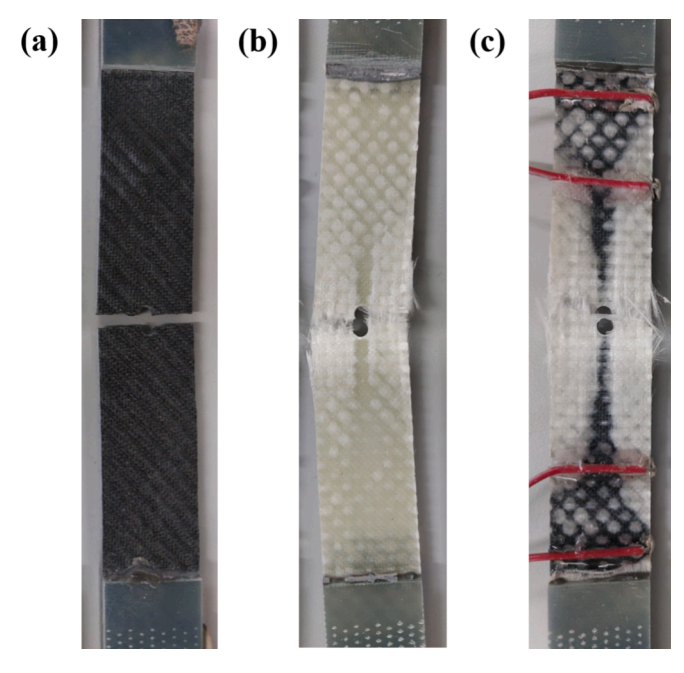


Fig. 7. Failure of open-hole specimens of (a) non-hybrid rCF composite, (b) non-hybrid E-glass fibre composite and (c) hybrid E-glass/rCF composite with a 3.2 mm-diameter hole after tensile testing.

other hole diameters.

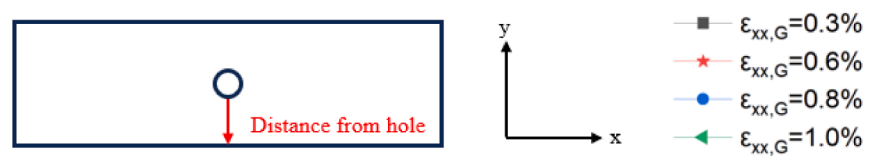
Both the unnotched specimens and the 3.2 mm diameter open-hole specimens of non-hybrid rCF composite failed in a very brittle manner, as evidenced by the sharp load drop in the stress-strain curves after the maximum load in Fig. 4. The fracture surface was clean and ran straight and flat in the transverse (width) direction, while for the openhole specimens it emanated transversely from the hole (Fig. 7a). The unnotched specimens gave a tensile strength of 175 MPa (compared to the strength of neat epoxy 54.5 MPa [20], showing that the presence of recycled carbon fibres does reinforce the epoxy giving three times increase in tensile strength. It has a failure strain of about 1.3 %. However, the random non-woven arrangement of the recycled carbon fibre showed significant material variability as reflected in the 11.3 % of coefficient of variation (c.v.) in its tensile strength measurement. When a 3.2 mm hole was introduced, the stress concentration at the hole caused the notched strength of the specimen to decrease by 35 % to 114 MPa (with a lower global strain at failure 0.8–0.9 %), but with a lower c. v. of 8.5 %. The reduction of c.v. can be explained by the fact that failure

was now localised and constrained to take place at the hole due to stress concentration instead of initiating at a random weakest point or defect within the larger volume of the gauge section. The brittle nature, low strain at failure and high material variability of the non-hybrid rCF non-woven composite suggests that it is not suitable to be used in isolation as a structural material. This motivates the subsequent investigation of its performance when it is hybridised with other reinforcement fibres.

The non-hybrid plain weave E-glass fibre composite gives an unnotched strength of 397 MPa (with failure strain around 2 %). It has a much lower material variability compared to the rCF non-woven composite due to its more structured plain weave woven fibre architecture. For the unnotched specimens, the failure is brittle and catastrophic considering the sharp load drop in the stress–strain curve in Fig. 5. However, for the open-hole specimens, the failure was more progressive. There was a small degree of localised delamination around the hole interacting with fibre failure (Fig. 7b), allowing slight stress redistribution and relief of stress concentration around the hole. This explains the rounded shape of their stress–strain curves near the peak load. The open-hole specimens of non-hybrid glass fibre composite demonstrated lower notch sensitivity compared to the rCF composite specimens, with the net strength retention of around 82–89 % for the range of hole diameters investigated.

The hybrid E-glass fibre/rCF composite has an unnotched strength of 300 MPa. For the unnotched specimens, damage firstly initiated in the low-strain rCF layer, followed by extensive delamination along the interfaces between the rCF layer and the woven glass fibre layer emanating from the initiation sites, before the ultimate glass fibre fracture. For the open-hole specimens, damage initiated in the rCF layer from the hole due to localised stress concentration, followed by delamination along the rCF-woven glass fabric interface in the ligaments adjacent to the holes, and finally glass fibre fracture took place next to the hole (Fig. 7c). The damage evolution will be described in detail in Section 3.2, where the damage monitoring functionality of the rCF layer is discussed. The presence of rCF non-woven layer and subcritical damage mechanism in the form of delamination helps redistribute the stress over a larger area, significantly blunting the stress concentration around the hole. The net stress-global strain curves in Fig. 6b for specimens of various hole sizes generally overlap with similar peak stresses and stress plateaus, suggesting that the hybrid composite is notchinsensitive. This is also supported by the net strength retention values of the notched specimens which are close to 100 %. Similar observation has also been reported in [21] for self-reinforced polypropylene where notch insensitivity was achieved by delamination in the material.

To further substantiate the role of rCF non-woven layer in facilitating load redistribution in the hybrid E-glass/rCF composite, the longitudinal strain ε_{xx} distribution across the ligament from the hole (see inset in Fig. 8) on the E-glass surface ply is extracted from the DIC analysis at four different global strain $\varepsilon_{xx,G}$ values (i.e. $\varepsilon_{xx,G} = 0.3$ %, 0.6 %, 0.8 % and 1.0 %) for the specimens of various hole diameters. This can reveal how the load is effectively distributed in the ligament next to the hole as the load is increased. It is then compared against the corresponding longitudinal strain distribution on the E-glass surface ply in the nonhybrid E-glass composite without the rCF non-woven layer at the same global strain values, as shown in Fig. 8. The results show that the strain gradient is generally more gradual with better strain uniformity in the hybrid E-glass/rCF composite, compared to the non-hybrid E-glass composite, especially for the open-hole specimens with small holes. At low strain (up to approximately 0.6 %), the strain distribution is more uniform due to the randomly orientated carbon fibres in the rCF nonwoven which help to disperse and redistribute the load across the ligaments. As the strain increases beyond 0.6 %, when damage is developed in the rCF non-woven layer at the hole, the glass fibre tows in the E-glass sublaminates next to the hole are then forced to carry more load and therefore the strain gradient near to the hole becomes steeper. However, the strain gradient is still more gradual compared to that of the nonhybrid glass fibre composite, demonstrating the load redistribution



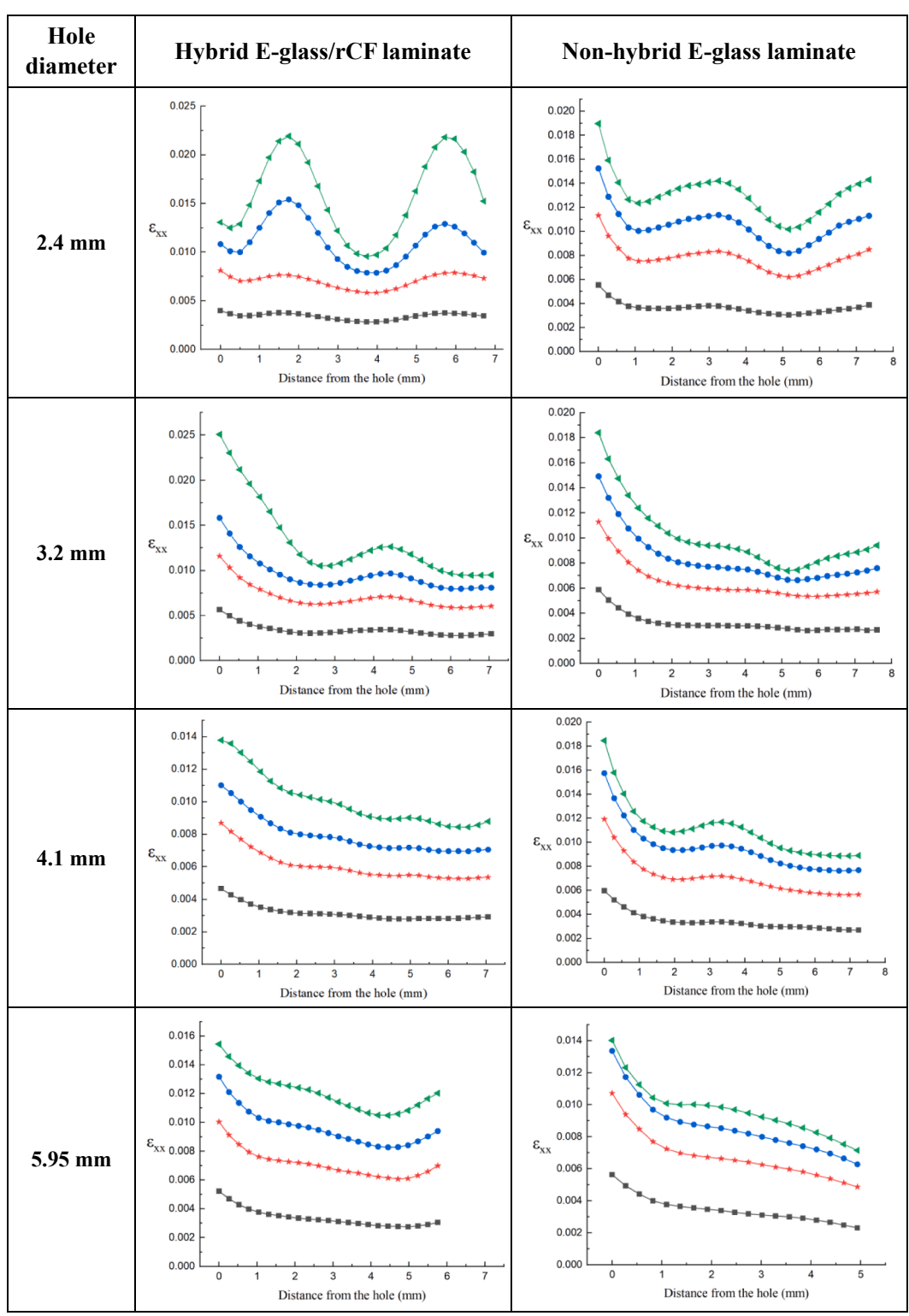


Fig. 8. Strain distribution in the ligament next to the hole at global strain $\varepsilon_{xx,G} = 0.3$ %, 0.6 %, 0.8 % and 1.0 % for four hole diameters in the hybrid E-glass/rCF laminate and non-hybrid E-glass fibre laminate.

capability of the remaining undamaged rCF non-woven layer. The waviness in the strain distribution plots seen in Fig. 8 reflects the woven pattern of the load-bearing E-glass fibre tows.

The use of orthotropic composites with holes can promote higher stress concentrations than their isotropic metallic counterparts [22], potentially leading to lower load bearing efficiency. This could have an impact in the overall weight and cost of the composite structure design. The gross strength retention versus diameter-to-width ratio for the three laminates is shown in Fig. 9, where their overall notch sensitivity can be compared. For a perfectly notch-insensitive material (such as a perfectly plastic material), the stresses are redistributed uniformly across the width and therefore its failure stress is proportional to the net section. This is represented by the ideal notch-insensitivity line in the figure. The hybrid rCF/glass fibre composite specimens follow closely the ideal notch-insensitivity line, followed by the pure glass fibre composite and the pure rCF composite which has the lowest open-hole strength retention. Although the hybrid composite seems to deviate slightly from the line as the holes get bigger, its notched strength under tensile loading can still be well approximated by simply using the ideal notchinsensitivity line. It makes the open-hole strength prediction of such composites straightforward, without the need for empirical measurement of characteristic length as in the point or average-stress criteria [23] in determining the notched strength, or for numerical methods such as advanced finite element analysis [24] which requires the full details of the hole geometry and high computational resources.

Note that the hybrid E-glass/rCF laminate has the same number of plies as in the non-hybrid E-glass laminate, except that the middle ply of the latter was replaced by a layer of rCF non-woven. The lower unnotched strength of the hybrid composite specimen (300 MPa) compared to that of the non-hybrid E-glass composite specimens (399 MPa) is attributed to the ply replacement with a thicker rCF non-woven mat which possesses a significantly low fibre volume fraction due to its non-optimised, non-aligned random fibre arrangement. However, when considering the load carrying capability of the non-hybrid E-glass fibre composite and the hybrid composite specimens, their ultimate failure load values are very close, as shown in Table 2. It is interesting to note that they are almost the same for all open-hole specimens. It implies that a 89 g/m² recycled carbon non-woven mat can be an economical substitute for a 270 g/m² E-glass woven fibre fabric in the middle of

laminate as the core material without compromising the overall load carrying capability of the laminate. Besides, it helps to improve the notch insensitivity of the woven glass fibre composite laminate by triggering large scale delamination not observed in a pure woven glass fibre composite. The thicker hybrid rCF/glass composite also means that it has better flexural rigidity and strength. However, there is an areal weight penalty of about 10 % as indicated in Table 1, which is tolerable for non-weight sensitive structural applications.

3.2. rCF for damage monitoring

The electrical conductivity of the load-bearing rCF can be exploited for a secondary function. In a non-woven arrangement, they form a complicated multi-directional fibre-fibre contact network whose electrical resistance can be responsive to the presence of strain and damage in the material, providing the possibility of real-time structural health monitoring. This section demonstrates the second functionality of rCF as a damage monitoring sensor in the open-hole hybrid rCF/glass fibre composite specimens with various hole sizes. The electrical resistance change in the rCF layer was measured to seek correlation to the extent of damage around the hole of the open-hole specimens. Two physical quantities on the external surface of the specimens were extracted from the DIC results as two independent means to indirectly indicate internal damage in the vicinity of the hole, i.e. the local strain ε_{xx} adjacent to the hole (averaged within ROI 1 and ROI 2 as indicated in Fig. 2) and the hole elongation measured from edge to edge across the hole. Fig. 10 shows the measurement of relative electrical resistance change ($\Delta R/R_0$) in the rCF layer for four representative open-hole specimens with hole diameters 2.4 mm, 3.2 mm, 4.1 mm and 5.95 mm respectively when subjected to monotonic tensile loading. It is plotted against global strain $\epsilon_{xx,G}$ which is measured near to the specimen edges away from the hole. Also shown in the same plot but separately are the local strains (Fig. 10 left) and the hole elongation (Fig. 10 right).

All the specimens present a consistent trend in the change of electrical resistance as they are loaded. Regardless of the hole diameter, the overall response of the hybrid composite specimen generally comprises three stages: undamaged linear elastic region (stage I), damage onset and propagation in the rCF layer (stage II) and delamination along the interface between the rCF layer and the woven glass fibre sublaminate

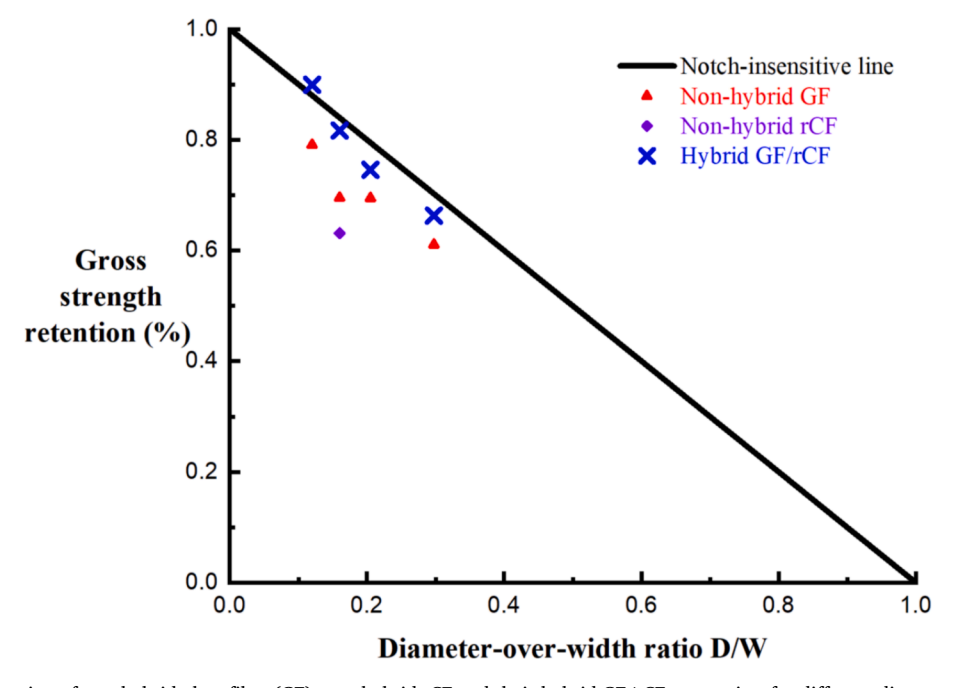


Fig. 9. Gross strength retention of non-hybrid glass fibre (GF), non-hybrid rCF and their hybrid GF/rCF composites for different diameter-over-width ratios (D/W). The ideal notch-insensitive line is also shown in the figure.

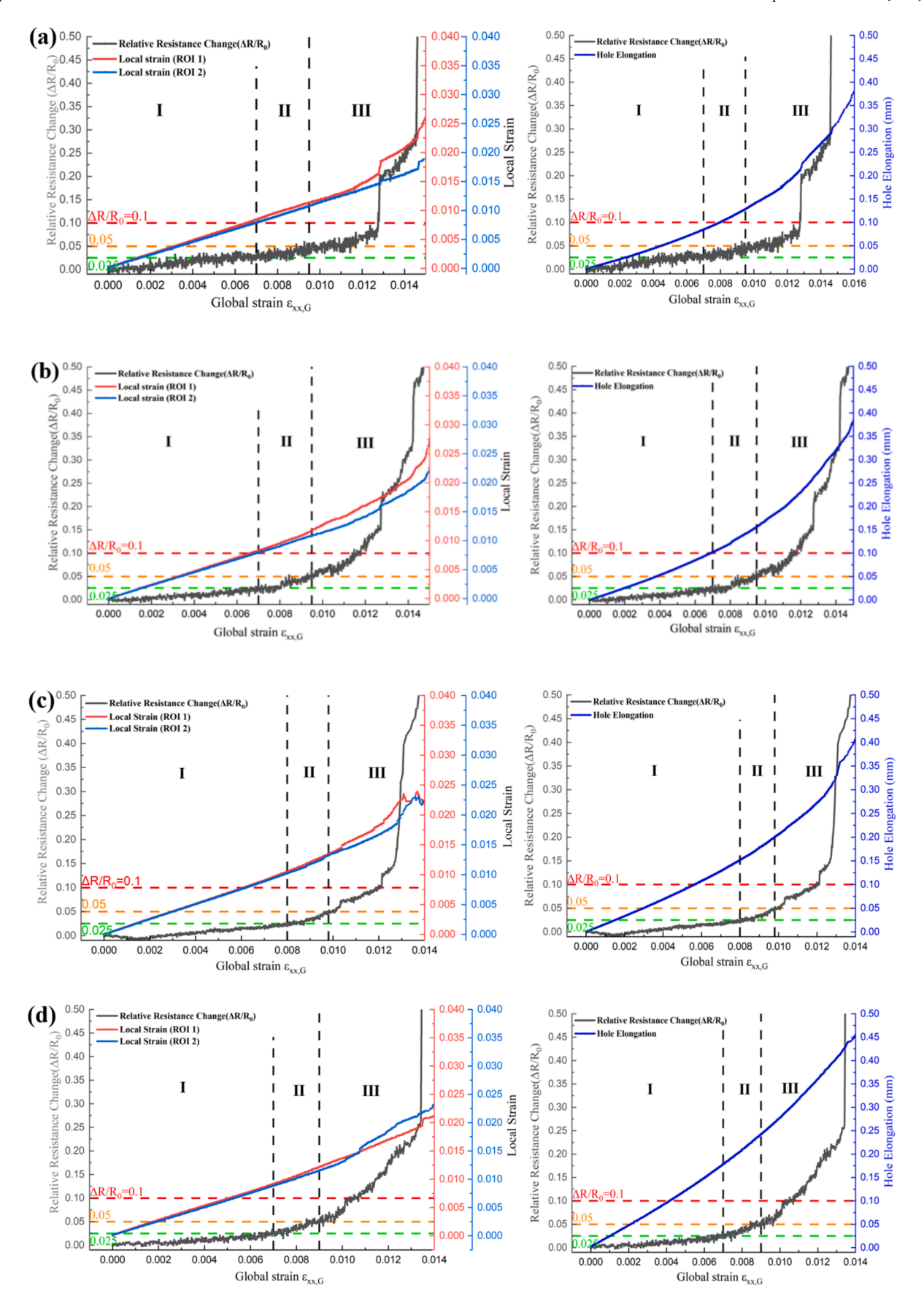


Fig. 10. (Left) Correlation between relative electrical resistance change ($\Delta R/R_0$) and local strains within the two ROIs on both sides of the hole, and (right) correlation between $\Delta R/R_0$ and hole elongation, for hole diameters (a) 2.4 mm, (b) 3.2 mm, (c) 4.1 mm, (d) 5.95 mm.

(stage III) (see Fig. 11). During stage I (up to global strain $\epsilon_{xx,G}$ about 0.7–0.8 %), the resistance change increases linearly due to combined elastic deformation of the carbon fibres in the rCF layer following tensile loading. As indicated in Fig. 11a, there is no detectable damage taking place around the hole, as confirmed by the overlapping local strain ϵ_{xx} measurements on both sides of the hole. The hole elongation curve also shows an approximately linear trend without a marked change in the slope.

In stage II (at global strain $\varepsilon_{xx,G}$ about 0.7 % to 0.95 %), upon further loading, damage or cracks are initiated in the rCF layer at both sides of the hole due to stress concentration and propagate in the width direction. As shown in Fig. 11b, there was appearance of white spots on the specimen surface due to localised straightening of the woven glass fibres of the surface ply, but it did not compromise the overall load carrying capability of the specimen. Closer inspection on the edge of the hole revealed cracks in the rCF layer, but no internal delamination was observed between the rCF layer and the glass fabric. Instead of failing in a brittle manner, the damage propagation in the rCF layer in the hybrid composite is more progressive as there are neighbouring glass fibre sublaminates constraining the opening of the cracks (in-situ effect [25]). Therefore, global strain up to 1 %, which is higher than the global strain at failure in the open-hole non-hybrid rCF composite (about 0.85 %, see Fig. 4), can be achieved. This is supported by the fact that there is finite reading from the electrical resistance measurement implying that the rCF layer has not completely failed upon reaching the global strain of 0.95 %. The damage propagation in stage II is also manifested in the change of the slope of the relative resistance change curve which becomes steeper and non-linear. At the same time, the local strains ε_{xx} on both sides of the hole start to deviate from each other, again confirming the presence of damage initiation at the hole in the rCF layer. The hole elongation curve also starts to display a steeper slope, indicating that the hole is becoming more elongated due to opening of the cracks next to the

Stage III (at global strain $\epsilon_{xx,G}$ about 0.95 % to 1.15 %) begins when delamination at the interface between rCF and woven glass fibre

sublaminate starts to take place at the damaged sites of the rCF layer. As the delamination propagates along the ligament of the specimen (Fig. 11c), the rCF layer is freed from the constraint imposed by the neighbouring glass fibre sublaminates, allowing the cracks in the rCF layer to further open up and propagate towards the edges of the specimen. This is shown by the rapid increase or step change in the electrical resistance reading. The local strains ε_{xx} within ROI 1 and ROI 2 continue to deviate apart, showing small asymmetry in the damage pattern of both sides of the hole due to local material variability caused by the randomly orientated rCF and the woven structure of the glass fabric. The hole elongation increases exponentially suggesting that the notch opening is now effectively larger. After the global strain $\varepsilon_{xx,G}$ of 1.4 %, the rCF layer fails completely when the electrical resistance increases sharply. The in-situ effect essentially allows the global strain of openhole rCF layer in the hybrid composite to go beyond that seen in the non-hybrid rCF composite, highlighting the benefit of hybridization of rCF with other continuous reinforcement fibres. Ultimately the hybrid composite fails by glass fibre fracture at global strain $\varepsilon_{xx,G}$ around 1.7 %, similar in value to that seen in the non-hybrid glass fibre composite. The fracture surface of the rCF layer was inspected using scanning electron microscopy (SEM), which reveals failure mechanisms such as fibre fracture and fibre pull-out (Fig. 12).

It is also interesting to demonstrate in Fig. 10 that, for all the hole sizes considered in this work, the demarcation of the three stages of the failure response in the hybrid composite can be commonly drawn using three constant $\Delta R/R_0$ lines at 2.5 %, 5 % and 10 % (represented by the green, amber and red lines respectively in Fig. 10). In practice, these threshold lines require calibration or adjustment for different composite laminates or lay-ups as their damage development is dependent on many factors such as ply thickness, ply orientation, type of fibre and matrix, type of loading, etc. This can be done via experimental testing or numerical modelling. Once it is calibrated, it can be developed into a simple green-amber-red warning or self-sensing system to inform the users of the level of damage and therefore the urgency for repair or part replacement, regardless of the size of the hole.

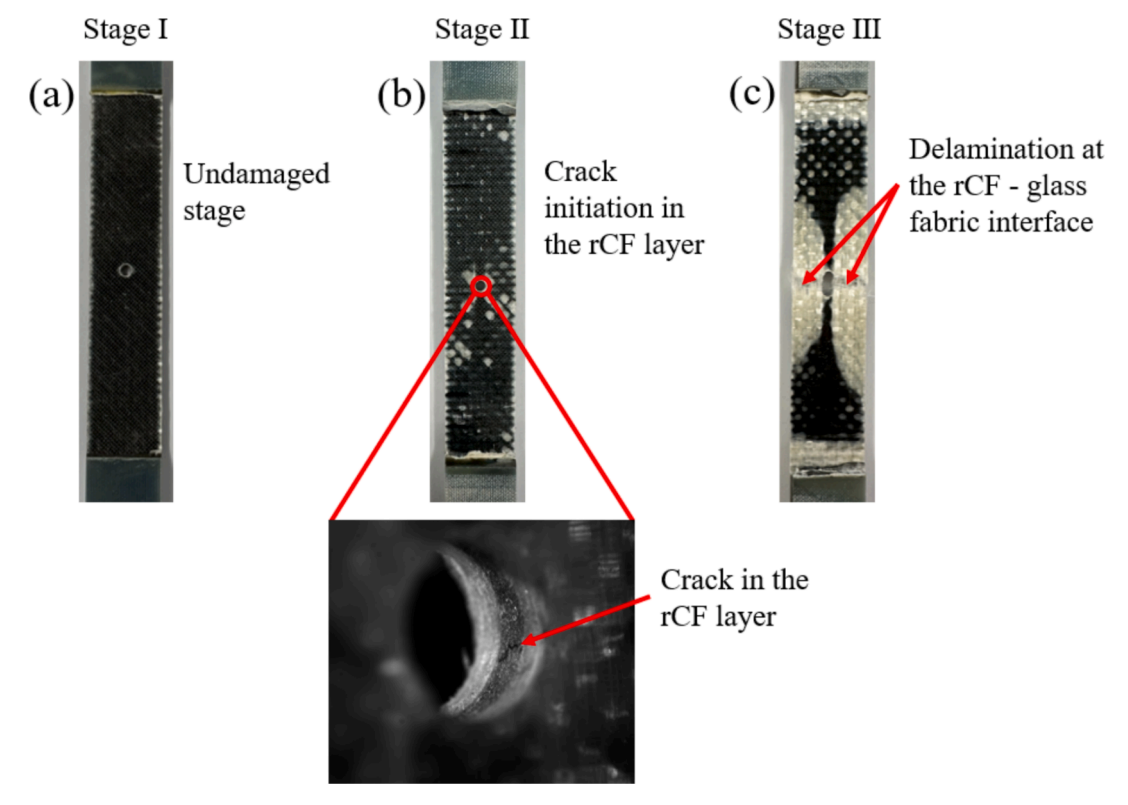


Fig. 11. The three stages of damage evolution in the hybrid rCF/glass composite specimen as the load is increased: (a) Stage I, (b) Stage II and (c) Stage III.

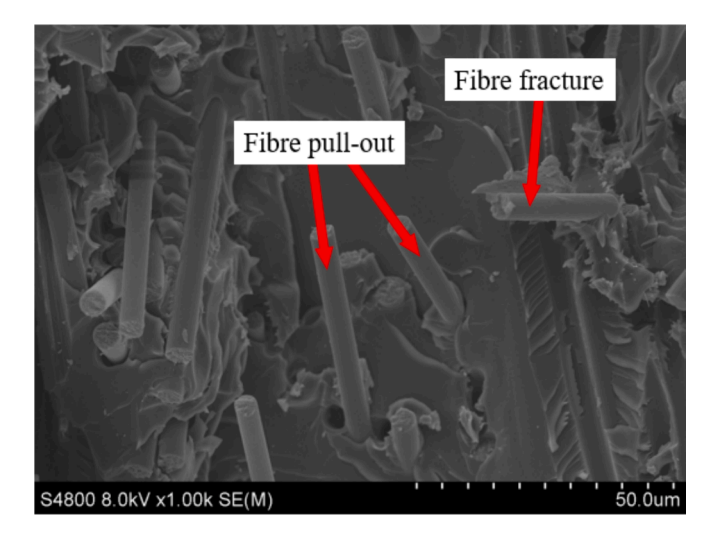


Fig. 12. SEM inspection of fracture surface of the rCF layer revealing failure mechanisms such as fibre fracture and fibre pull-out.

Composites commonly fail at holes or notches due to stress concentrations. However, it is challenging to peer into the interior of the material and inspect for internal damage around holes, especially when they are filled with fasteners. The results suggest that a damage selfsensing hybrid composite can be developed by adding a thin rCF layer for monitoring the structural health of a holed composite structure insitu and in real time. This overcomes the disadvantages of using embedded sensors which can be a stress raiser affecting the mechanical strength of the structure and requires complex manufacturing processes. In this case, the composite material constituent itself, i.e. the rCF layer, which is an integral part of the composite structure is used as a sensor. Furthermore, the sensing can be done using an inexpensive multimeter. To the authors' knowledge, there is no extensive study being done on the piezoresistivity or sensing performance of carbon fibre non-woven mats. The extensive network of the non-aligned random fibre-fibre contact in a non-woven mat could offer some advantages in damage monitoring capability when compared to the aligned continuous fibre arrangement, for example in a unidirectional ply [26-28] or a woven fabric [29]. It is sensitive enough to pick up matrix failure which typically takes place very early on before the ultimate fibre failure. The non-directionality and high drapability of the non-woven arrangement also enable damage sensing coverage over a large volume of a complex composite component. Probing electrodes can be placed at any convenient locations around the hole or notch due to its isotropic electrical conductivity without the requirement to follow certain fibre orientation. For instance, it could work by placing the electrodes at the edges of the composite part, as demonstrated in this work. In Fig. 10, it is also interesting to note that the slopes of the relative resistance change $\Delta R/R_0$ against global strain $\varepsilon_{xx,G}$ are similar for all hole diameters at low strain up to 0.8 % where the material behaves linearly. They have a common slope or gauge factor of about 3.1, similar in magnitude to the gauge factor of a metal foil strain gauge (typically around 2). This means the rCF layer can potentially also be used as a strain sensor, which will be the subject of subsequent investigation.

As with most sensors, exposure of the rCF layer to the environmental changes (e.g. temperature and humidity) can influence its sensing reliability. In this work, the damage sensing rCF layer was embedded as the mid-ply of the laminate such that its exposure to environmental agents was minimised. Therefore, this work focusses mainly on the damage monitoring performance of the rCF layer solely due to mechanical loading. The investigation of the effects of environmental exposure on the sensing performance of the rCF layer is beyond the scope of this paper.

4. Conclusions

The pure rCF non-woven composites cannot be used in isolation for structural applications. They are not damage tolerant and their strength is highly sensitive to notches. In this study, a single rCF non-woven layer was hybridised with woven glass fabrics as a core material to explore its multi-functionality in an open-hole configuration under monotonic tensile loading. It was found to exhibit notch insensitive behaviour due to the presence of the rCF non-woven and the occurrence of sub-critical delamination along the interfaces between the rCF and glass fibre layers, enabling redistribution of the stresses around the holes. The in-situ effect provided by the neighbouring glass fibre sublaminates allows the rCF layer to be loaded beyond the strain at failure of a stand-alone pure rCF composite and failed in a more progressive manner. Through monitoring the electrical resistance changes in the rCF layer during tensile loading, it is possible to provide indication on the three key damage stages in the hybrid composite, i.e. undamaged stage, damage initiation and propagation in the rCF layer, and delamination along the rCF and glass fibre interfaces. It paves the way for a development of a multi-functional rCF layer in a hybrid composite by offering the mechanical function in reducing stress concentration around an open hole or notch, and the damage (structural health) monitoring function through measurement of electrical resistance change. There is scope for further investigation in the use of rCF non-woven as a strain sensor and its reliability under cyclic loading.

CRediT authorship contribution statement

Fan Zhang: Writing – review & editing, Writing – original draft, Visualization, Methodology, Formal analysis, Data curation, Conceptualization. Ting Yang Ling: Supervision, Project administration, Funding acquisition, Conceptualization. Liudi Jiang: Writing – review & editing, Supervision, Project administration. Yonggang Zhang: Supervision, Resources, Project administration, Funding acquisition. Khong Wui Gan: Writing – review & editing, Writing – original draft, Supervision, Methodology, Funding acquisition, Conceptualization.

Declaration of competing interest

The authors declare that they have no known competing financial interests or personal relationships that could have appeared to influence the work reported in this paper.

Acknowledgement

This work is supported by the Fundamental Research Grant Scheme (FRGS/1/2019/TK09/USMC/02/1) of the Ministry of Higher Education of Malaysia and the University of Southampton Malaysia (UoSM) PhD Studentship.

Data availability

The raw/processed data required to reproduce these findings are available upon request from the corresponding author.

References

- Song YS, Youn JR, Gutowski TG. Life cycle energy analysis of fiber-reinforced composites. Compos A Appl Sci Manuf Aug. 2009;40(8):1257–65. https://doi.org/ 10.1016/j.compositesa.2009.05.020.
- [2] J. Zhang, V. S. Chevali, H. Wang, and C. H. Wang, "Current status of carbon fibre and carbon fibre composites recycling," Jul. 15, 2020, Elsevier Ltd. 10.1016/j. compositesb 2020 108053
- [3] Yaw Attahu C, Ket Thein C, Wong KH, Yang J. Enhanced damping and stiffness trade-off of composite laminates interleaved with recycled carbon fiber and short virgin aramid fiber non-woven mats. Compos Struct 2022;297:Oct. https://doi. org/10.1016/j.compstruct.2022.115981.

- [4] Koçoğlu H, Kodal M, Altan MC, Özçelik B, Özkoç G. A new approach for the reuse of scrap carbon fiber in high-added value continuous fiber reinforced composite structures. Compos A Appl Sci Manuf Dec. 2022;163. https://doi.org/10.1016/j. compositesa 2022 107272
- [5] Quan D, Farooq U, Zhao G, Dransfeld C, Alderliesten R. Recycled carbon fibre mats for interlayer toughening of carbon fibre/epoxy composites. Mater Des Jun. 2022; 218. https://doi.org/10.1016/j.matdes.2022.110671.
- [6] A. Danish et al., "Utilization of recycled carbon fiber reinforced polymer in cementitious composites: A critical review," Aug. 01, 2022, Elsevier Ltd. 10.1016/j. jobe.2022.104583.
- [7] Akbar A, Liew KM. Assessing recycling potential of carbon fiber reinforced plastic waste in production of eco-efficient cement-based materials. J Clean Prod Nov. 2020;274. https://doi.org/10.1016/j.jclepro.2020.123001.
- [8] de Souza Abreu F, Ribeiro CC, da Silva Pinto JD, Nsumbu TM, Buono VTL. Influence of adding discontinuous and dispersed carbon fiber waste on concrete performance. J Clean Prod 2020;273:Nov. https://doi.org/10.1016/j. iclapro 2020 122220
- [9] Mastali M, Dalvand A, Sattarifard A. The impact resistance and mechanical properties of the reinforced self-compacting concrete incorporating recycled CFRP fiber with different lengths and dosages. Compos B Eng Mar. 2017;112:74–92. https://doi.org/10.1016/j.compositesb.2016.12.029.
- [10] Segura I, Faneca G, Torrents JM, Aguado A. Self-sensing concrete made from recycled carbon fibres. Smart Mater Struct 2019;28(10):Sep. https://doi.org/ 10.1088/1361-665X/ab3d59.
- [11] Belli A, Mobili A, Bellezze T, Tittarelli F. Commercial and recycled carbon/steel fibers for fiber-reinforced cement mortars with high electrical conductivity. Cem Concr Compos May 2020;109. https://doi.org/10.1016/j. cemconcomp.2020.103569.
- [12] Hu Q, Duan Y, Zheng X, Nie W, Zou L, Xu Z. Lightweight, flexible, and highly conductive recycled carbon fiber felt for electromagnetic interference shielding. J Alloy Compd Feb. 2023;935. https://doi.org/10.1016/j.jallcom.2022.168152.
- [13] Meng F, McKechnie J, Pickering SJ. An assessment of financial viability of recycled carbon fibre in automotive applications. Compos A Appl Sci Manuf Jun. 2018;109: 207–20. https://doi.org/10.1016/j.compositesa.2018.03.011.
- [14] Balaji AB, Rudd C, Liu X. Recycled Carbon Fibers (rCF) in automobiles: Towards Circular Economy. Mater Circ Econ 2020;2(1):Dec. https://doi.org/10.1007/ s42824-020-00004-0.
- [15] Longana ML, Yu HN, Jalavand M, Wisnom MR, Potter KD. Aligned discontinuous intermingled reclaimed/virgin carbon fibre composites for high performance and pseudo-ductile behaviour in interlaminated carbon-glass hybrids. Compos Sci Technol May 2017;143:13–21. https://doi.org/10.1016/j. compscitech.2017.02.028.
- [16] Gan KW, Ho YW, Ow ZY, Israr HA, Wong KJ. Aligned discontinuous carbon fibre tows in hybrid composites and their tensile behaviour: an experimental study.

- J Compos Mater Nov. 2019;53(26–27):3893–907. https://doi.org/10.1177/0021998319849697.
- [17] Liu Z, Turner TA, Wong KH, Pickering SJ. Development of high performance recycled carbon fibre composites with an advanced hydrodynamic fibre alignment process. J Clean Prod Jan. 2021;278. https://doi.org/10.1016/j. iclepro.2020.123785.
- [18] Wölling J, Schmieg M, Manis F, Drechsler K. Nonwovens from Recycled Carbon Fibres – Comparison of Processing Technologies. Procedia CIRP Jan. 2017;66: 271–6. https://doi.org/10.1016/J.PROCIR.2017.03.281.
- [19] Pakdel E, Kashi S, Varley R, Wang X. Recent progress in recycling carbon fibre reinforced composites and dry carbon fibre wastes. Resour Conserv Recycl Mar. 2021;166:105340. https://doi.org/10.1016/J.RESCONREC.2020.105340.
- [20] "EpoxAmiteTM 103 Product Information | Smooth-On, Inc." Accessed: Jul. 02, 2025. [Online]. Available: https://www.smooth-on.com/products/epoxamite-103/.
- [21] Nijs A, et al. Notch-sensitivity of hybrid carbon-fibre/self-reinforced polypropylene composites. Compos Sci Technol Nov. 2020;200. https://doi.org/10.1016/j. compscitech.2020.108422.
- [22] Zappalorto M, Carraro PA. An engineering formula for the stress concentration factor of orthotropic composite plates. Compos B Eng Jan. 2015;68:51–8. https:// doi.org/10.1016/J.COMPOSITESB.2014.08.020.
- [23] Whitney JM, Nuismer RJ. Stress Fracture Criteria for Laminated Composites Containing stress Concentrations. J Compos Mater 1974;8(3):253–65. https://doi. org/10.1177/002199837400800303.
- [24] Camanho PP, Lambert M. A design methodology for mechanically fastened joints in laminated composite materials. Compos Sci Technol Dec. 2006;66(15):3004–20. https://doi.org/10.1016/j.compscitech.2006.02.017.
- [25] Camanho PP, Dávila CG, Pinho ST, Iannucci L, Robinson P. Prediction of in situ strengths and matrix cracking in composites under transverse tension and in-plane shear. Compos A Appl Sci Manuf Feb. 2006;37(2):165–76. https://doi.org/ 10.1016/j.compositesa.2005.04.023.
- [26] Angelidis N, Wei CY, Irving PE. The electrical resistance response of continuous carbon fibre composite laminates to mechanical strain. Compos A Appl Sci Manuf Oct. 2004;35(10):1135–47. https://doi.org/10.1016/j.compositesa.2004.03.020.
- [27] J. C. Abry, Y. K. Choi, A. Chateauminois, B. Dalloz, G. Giraud, and M. Salvia, "Insitu monitoring of damage in CFRP laminates by means of AC and DC measurements." [Online]. Available: www.elsevier.com/locate/compscitech.
- [28] Swait TJ, Jones FR, Hayes SA. A practical structural health monitoring system for carbon fibre reinforced composite based on electrical resistance. Compos Sci Technol Aug. 2012;72(13):1515–23. https://doi.org/10.1016/j. compscitech.2012.05.022.
- [29] Alsaadi A, Meredith J, Swait T, Curiel-Sosa JL, Hayes S. Damage detection and location in woven fabric CFRP laminate panels. Compos Struct Jul. 2019;220: 168–78. https://doi.org/10.1016/j.compstruct.2019.03.087.